

A Monte Carlo Platform for Characterization of X-Ray Radiation Dose in CT Imaging

Delaram Pakravan¹, Farshid Babapour Mofrad^{2*}, Mohammad Reza Deevband³, Mahdi Ghorbani³, Hamidreza Pouraliakbar⁴

ABSTRACT

Background: Computed tomography (CT) is currently known as a versatile imaging tool in the clinic used for almost all types of cancers. The major issue of CT is the health risk, belonging to X-ray radiation exposure. Concerning this, Monte Carlo (MC) simulation is recognized as a key computational technique for estimating and optimizing radiation dose. CT simulation with MCNP/MCNPX MC code has an inherent problem due to the lack of a fan-beam shaped source model. This limitation increases the run time and highly decreases the number of photons passing the body or phantom. Recently, a beta version of MCNP code called MCNP-FBSM (Fan-Beam Source Model) has been developed to pave the simulation way of CT imaging procedure, removing the need of the collimator. This is a new code, which needs to be validated in all aspects.

Objective: In this work, we aimed to develop and validate an efficient computational platform based on modified MCNP-FBSM for CT dosimetry purposes.

Material and Methods: In this experimental study, a setup is carried out to measure CTDI₁₀₀ in air and standard dosimetry phantoms. The accuracy of the developed MC CT simulator results has been widely benchmarked through comparison with our measured data, UK's National Health Service's reports (known as ImPACT), manufacturer's data, and other published results.

Results: The minimum and maximum observed mean differences of our simulation results and other above-mentioned data were the 1.5%, and 9.79%, respectively.

Conclusion: The developed FBSM MC computational platform is a beneficial tool for CT dosimetry.

Citation: Pakravan D, Babapour Mofrad F, Deevband MR, Ghorbani M, Pouraliakbar H. A Monte Carlo Platform for Characterization of X-Ray Radiation Dose in CT Imaging. *J Biomed Phys Eng*. 2021;11(3):271-280. doi: 10.31661/jbpe.v0i0.2012-1254.

Keywords

Tomography, X-Ray Computed; Monte Carlo Method; Dosimetry; Fan-beam CT; System performance

Introduction

The fan-beam computed tomography (CT) scanners are the most common CT scanners in the clinical environment. Lead collimator is used to make fan-shaped beam geometry [1]. Examinations with X-ray CT is rapid, and accessible to 24 h a day, and is also utilized for approximately all patients and bodily cancers [2]. However, it delivers a relatively high dose to the patient, mostly greater than 10 mSv effective doses for each examination [3]. Unavoidable radiation exposure is the perennial disadvantage of CT imaging, which is proliferating because of the accessibility and frequency of this examination. To address

¹PhD Candidate, Department of Medical Radiation Engineering, Science and Research Branch, Islamic Azad University, Tehran, Iran

²PhD, Department of Medical Radiation Engineering, Science and Research Branch, Islamic Azad University, Tehran, Iran

³PhD, Department of Biomedical Engineering and Medical Physics, School of Medicine, Shahid Beheshti University of Medical Sciences, Tehran, Iran

⁴PhD, Rajaie Cardiovascular Medical and Research Center, Iran University of Medical Sciences, Tehran, Iran

*Corresponding author: Farshid Babapour Mofrad
Department of Medical Radiation Engineering, Science and Research Branch, Islamic Azad University, Tehran, Iran
E-mail: Farshid.mofrad@yahoo.com

Received: 27 December 2020
Accepted: 20 February 2020

this issue, estimation of the radiation dose and minimization of the radiation exposure are an essential steps for clinical routines.

Monte Carlo (MC) method is the most trustworthy approach to estimate and characterize dose values in CT imaging [4]. The most common international MC codes for simulation of real procedures in the field of medical radiation physics include MCNP [5], GEANT [6], FLUKA [7], and EGSnrc [8]. Kostou et al. [9] developed a CT simulator for dosimetry purposes using GATE (GEANT4 Application for Tomographic Emission) code, based on GEANT4. Keramer et al. [10] devised mathematical modeling of bowtie filters using a sigmoid Boltzmann function for an EGSnrc based-MC CT dosimetry. Somasundaram et al. [11] developed an open-source MC CT dosimetry model using Fluka code. Akhavanallaf et al. [12] developed an MCNP-based MC CT simulator for assessing in-phantom CT dose uncertainties. The primary step in the MC modeling of such scanners is the X-ray source simulation, where all of these codes are not optimized enough due to the lack of an optimized CT source model, removing the needs of the collimator for shaping beam into fan geometry [13]. This problem has fatally affected the execution time of MC simulation, accuracy and precision of outcomes [12, 13]. X-ray photons come from a bimodal focal spot profile [14] on the anode area, and then their directions are trimmed into fan geometry by lead leaves of the collimator. This routine/standard approach increases fatally run-time because photon particles interact with collimator jaws and then are absorbed or secondary particles like electrons and low-energy photons are generated. To overcome this problem, source biasing technique is proposed to decrease the contribution of incoming photons in the outside of the field-of-view. There are at least three ways proposed to simulate a fan-beam CT source model in the MCNP code, including standard method, the cookie-cutter technique, and a bunch of pencil beams

comprising many discrete point sources [13]. The only realistic estimation of reality is the standard source model, which is time-consuming even using source biasing [13] and thus to overcome the problem of particle starvation imposed by the collimator, a fan-beam CT source model called “MCNP-FBSM” has been proposed for calculation of imaging parameters [13]. However, the accuracy of this code has not been examined by dosimetry parameters. Moreover, this code is not appropriated for CT dosimetry applications because of the lack of bowtie filters. Therefore, the main contributions of the present study can be highlighted as follows:

- Development of the MCNP-FBSM MC software package by the implementation of bowtie filters.
- Experimental measurements of free-in-air Computed Tomography Dose Index (CTDI), and both head and body phantom waited CTDI (CTDI_w) values.
- An extensive validation of our CT simulator through the comparisons with our experimental results and a wide range of previously published reference data [15-17].

Material and Methods

Specifications of used CT scanner

In this experimental study, a volumetric 64-slice GE LightSpeed™ VCT scanner (GE Healthcare Technologies, Waukesha, WI) was simulated using MCNP code for data acquisition. The specification of this scanner was presented in Table 1 [16, 18].

Development of a Monte Carlo platform for characterization of X-ray radiation dose and modeling of the CT system

MCNP-FBSM Monte Carlo Code

The general-purpose Monte Carlo N-Particle radiation transportation (MCNP) code [19] was developed to use in various scientific fields, especially for application in medi-

Table 1: Details of the experimental scan parameters to perform free-in-air computed tomography dose index measurements.

Scan Type	Axial
Source-to-image detector distance (mm)	950
Source-to-isocenter distance (mm)	540
Fan angle (degrees)	56
Tube voltage (kVp)	120
Anode-inherent and additional filter (mm)	W-Al (3.25) and Cu (0.1)
Tube current-time product (mAs)	350
Slice thickness (mm)	40
No. of channels	64
Channel width (mm)	0.625
Bowtie filter	Small, Large

cal physics. However, an effective fan-beam source model for simulation of clinical CT scanner is still missing. Therefore, it has recently been devised and implemented in the subroutines of the MCNP code, which yielded a proper MCNP MC code for CT imaging called MCNP-FBSM [13]. MCNP-FBSM was designed to transport particle types present in the CT procedure, including photon and electron over a wide range of energies. The photoelectric and Compton cross sections are based on Storm and Israel [20], and ENDF (Evaluated Nuclear Data File) tabulations [21], respectively. The Klein-Nishina cross-section in Compton scattering is modified by the electron binding effect. The state-of-the-art photon cross-section library, *mcplib04*, was utilized. This photon library is according to the EPDL97 [22]. Although the MCNP-FBSM was developed for CT imaging applications, the implementation of bowtie filters is still missed in the MCNP-FBSM MC code. Thus, it is not reliable enough to estimate radiation dose in the CT procedure. In this work, we

aimed to develop an MC CT simulator-based MCNP-FBSM for characterization of X-ray radiation dose and modeling of the CT system for CT dosimetry purposes. In the following, we attempt to address the details of this developed CT simulator.

X-Ray Source and X-ray Spectra Simulation

The X-ray source was simulated according to the information in Table 1. In this study, to improve the efficiency of Monte Carlo simulation, the anode of the X-ray tube was assumed as a point source, emitting the X-ray photons. There are several tools for generating X-ray spectra like MamSim [23], SPEKTR [24], TASMIP [25], and IPEM [26]. In this study, the IPEM software package [26] was used to generate X-ray spectra. According to Table 1, the X-ray generated from a tungsten target is estimated by the Birch and Marshall (B & M) program [27], which is the basis of the IPEM Report 78 catalog of X-ray spectra. The 80 kV, 100 kV, 120 kV, and 140 kV spectra were calculated with a tungsten anode and anode angle of 7° and a 3.25 mm aluminum and 0.1 mm copper filter. The X-ray source moves along a single axial, contiguous axial or helical axial trajectory during a CT procedure. Similar to the work of Gu et al. [28], in this study, 18 X-ray sources with the 20-degree angular difference were considered around the phantom to approximate the source motion in a 360-degree full rotation.

Simulation of bowtie filters

The aim of bowtie filters in CT imaging is to make uniform the X-ray intensity acquired by the detectors in order to amend the image quality and meantime to diminish the dose to the patient due to the privileged filtering about the periphery of the fan beam. It is significant to take the result of bowtie filters into account for CT dosimetry, and mainly for MC simulations of absorbed doses to patients [29]. In this study, head and body bowtie filters were used. The bowtie filters, shown in Figure 1, were simulated based on directly measured data.



Figure 1: A representation of the bowtie filter module along with its Aluminum holder used in the General Electric LightSpeed™ Volume Computed Tomography scanner.

Due to the unwillingness of the manufacturer to disclose the proprietary information, we avoided mentioning geometrical dimensions and the material composition of bowtie filters.

CTDI Phantoms

In this study, standard head, and body phantoms were utilized. These two phantoms are made of polymethyl methacrylate (PMMA) with a density of 1.19 g.cm^{-3} . The diameter of the head and body phantoms were 16 cm and 32 cm, respectively. The length of both phantoms was 15 cm. Each phantom has 5 holes with dimensions of 15 cm in length and 10 mm in diameter. Each phantom consists of four peripheral cavities in the positions of 12, 3, 6, and 9 o'clock positions, and one cavity in the center. The distance of each peripheral hole from the edge of the phantom is 1 cm. These holes are installed to place the pencil ionization chamber.

Monte Carlo Simulation of CT dosimetry parameters

Estimation of radiation dose in CT imaging systems is very important in quality control/quality assurance procedures and CTDI is a standard parameter in CT dosimetry [17, 30]. Regarding EUR 16262 [31], the $CTDI_w$ metric is calculated as follows:

$$CTDI_w = \frac{2}{3}CTDI_{100, \text{peripheral}} + \frac{1}{3}CTDI_{100, \text{center}} \quad (1)$$

Where $CTDI_{100, \text{center}}$ and $CTDI_{100, \text{peripheral}}$ parameters are the center and peripheral CTDI. These parameters are measured by ion-cham-

ber, which is the same condition applied in the simulation. Due to the low electron density of air, photon interactions are less frequent. To accelerate MC simulation of $CTDI_{100}$ parameter, PMMA material was used instead of air into the ion-chamber and then transferred to the air via a conversion factor (CF) as follows [10]:

$$D_{air} = D_{PMMA} \times CF \quad (2)$$

Where CF is calculated as follows:

$$CF = \frac{\sum_E \Phi(E) \left(\frac{\mu_{en}(E)}{\rho} \right)_{air}}{\sum_E \Phi(E) \left(\frac{\mu_{en}(E)}{\rho} \right)_{PMMA}} \quad (3)$$

Where $\Phi(E)$, $\left(\frac{\mu_{en}(E)}{\rho} \right)_{air}$, and $\left(\frac{\mu_{en}(E)}{\rho} \right)_{PMMA}$ are photon fluence spectrum, mass-energy absorption coefficients for air, and PMMA, respectively. The absorption coefficients were taken from the X-ray data published on the website of the National Institute of Standards and Technology (NIST) [32]. D_{PMMA} has been estimated utilizing the F6 (in MeV/cm²/source particle history) tally. FM card was used for applying the results of dividing the numerator and denominator values of Eq. (3) to D_{PMMA} . It should be noted that the MCNP tally values are normalized per source particle history as mentioned above. Consequently, the determination of the absorbed dose from MC simulation for CT procedure should be converted to

the absorbed dose with a practical routine unit (mGy/100 mAs), and subsequently, $CTDI_{100}$ was calculated from D_{air} as follows:

$$CTDI_{100} = D_{air} \times \frac{CTDI(E, ST)_{100, air, measured \text{ per } 100 \text{ mAs}}}{CTDI(E, ST)_{100, air, simulated \text{ per } particle}} \quad (4)$$

Where E and ST are energy and slice thickness, respectively. To validate the simulated $CTDI_{100}$ values, the same setup, which carried out for experimental and reference measurements, was used in the MC simulations. The number of source photons was 50 million. The MC computations were carried out on a Core™ i5 PC with a 2.5 GHz processor and 4 Gbytes of RAM.

Benchmarking

In order to benchmark the accuracy of the developed CT simulator in the MC simulation of radiation dose in the CT procedure, a set of simulations was performed. The simulations mimicked the system parameters given in Table 1, which are used by ImpACT [15], GE manufacturer's data [16], and other published reference results [17]. ImpACT data [15] were available under the various tube voltages, including 80 kVp, 100 kVp, 120 kVp, and 140 kVp and different range slice thicknesses from

1.25 mm to 40 mm. GE manufacturer's data [16], and other published reference results [17] were unitedly available under the system parameters indicated in Table 1. Moreover, we performed a set of experimental measurements under the same setup mentioned in Table 1, as given in the following.

The dose monitoring was carried out by a typical ion-chamber (PTW, Model TW30009), coupled to an electrometer (PTW, Model Unidos E). The chamber consists of a shell and a cylindrical air cavity. The chamber is 10 cm in length and 10 mm in diameter. This chamber is made of PMMA with 1 mm wall thickness and cylindrical air volume with 8 mm diameter. As shown in Figure 2, in order to CT output monitoring, the ionization chamber is firstly placed in free-in-air at gantry iso-center and then $CTDI_{100, air}$ was determined. To read and record the CTDI in the phantom, standard CTDI body and head phantoms were used and ion-chamber is placed in one of the five holes each time, and four PMMA filler rods are placed in the rest of the vacant holes as illustrated in Figure 2 and according to Eq. (1), $CTDI_w$ determined. Experimental radiation dose measurements were repeated ten times to reach an adequate precision [30].

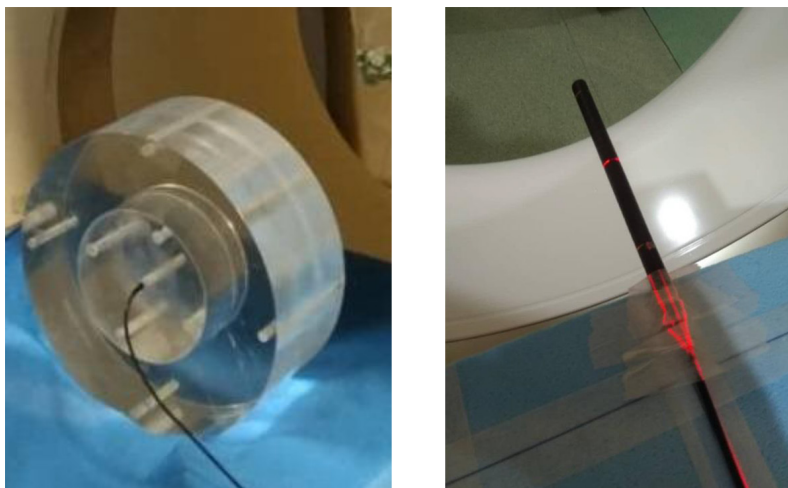


Figure 2: A representation of the standard/routine dosimetry phantoms (a) and a 10 cm pencil ionization chamber (b) used for measurements of X-ray computed tomography dose and radiation exposure, respectively.

Results

In this part, first, the comparison of the results of the CT simulator and ImpACT [15] has been made under the various tube voltages in the range of 80-140 kVp and different slice thicknesses in the range of 1.25-40 mm. Second, the simulated results have been compared with our experimental data, the references [15-17] under the same protocol mentioned in Table 1.

Figure 3 (a) displays the estimated unfiltered X-ray spectra with tungsten anode for various constant tube voltages, including 80 kV, 100 kV, 120 kV, and 140 kV supplied from IPEM-78 software package [26]. Figure 3 (b) illustrates the calculated CF using Eq. 3 as a function of various energy bins. This ratio converts the PMMA dose to air one, accelerating the process of the MC simulations.

Figure 4 demonstrates mean free-in-air CTDI values as a function of different tube potentials and slice thicknesses for (a) small bowtie filter, and (b) large bowtie filter, while (c), and (d), respectively, show head and body CTDI values as a function of various tube voltages and beam widths. These results were compared with the reference data [15]. The simulated data, which were acquired by the developed X-ray CT simulator, display 4.2%

difference, averaged across all CTDI values.

Table 2 demonstrates mean free-in-air CTDI and head and body phantom CTDI values and their relevant standard deviations obtained under the exposure condition indicated in Table 1, comparing our results and other previously published data [15-17]. The simulated results in comparison with the experimental data and other studies [15-17] show the average of differences 4.28%, 2.53%, 9.79%, and 1.5%, respectively.

Discussion

MC method is the most reliable approach to characterize CT dose values [4]. The most common MC codes are MCNP [5], GEANT [6], FLUKA [7], and EGSnrc [8]. None of these codes are optimized enough because of the lacking an optimized fan-beam CT source model [13]. This strongly decreases the efficiency of MC programs and the number of tracking photons [12, 13]. To solve these problems, a new MC code called “MCNP-FBSM” has been proposed for the calculation of imaging parameters [13]. However, this code is not for CT dosimetry applications because of the lack of bowtie filters. Moreover, the accuracy of this code has not been checked for dosimetry parameters. Therefore, in this study, the

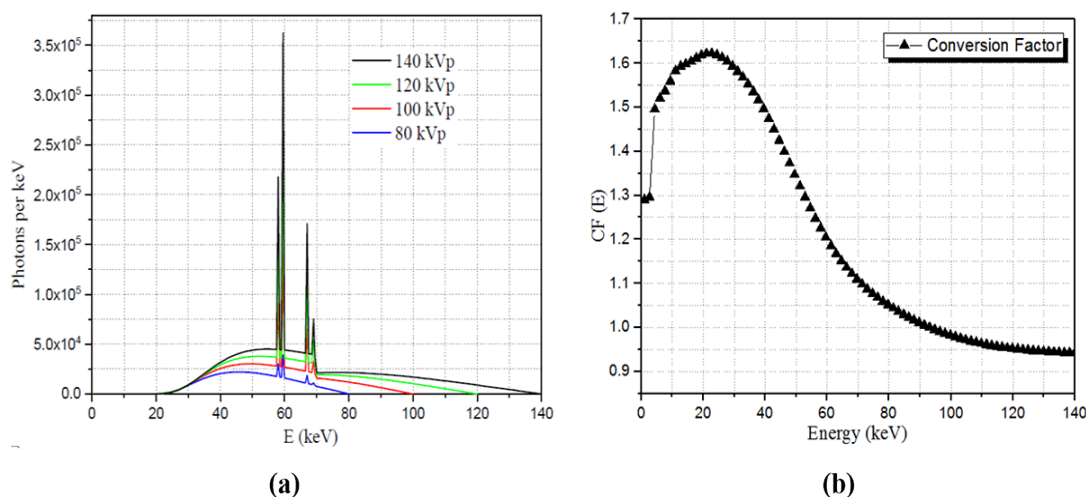


Figure 3: Calculated (a) filtered X-ray spectra for different tube potentials, (b) the conversion factor as a function of photon energy for transferring polymethyl methacrylate to air dose.

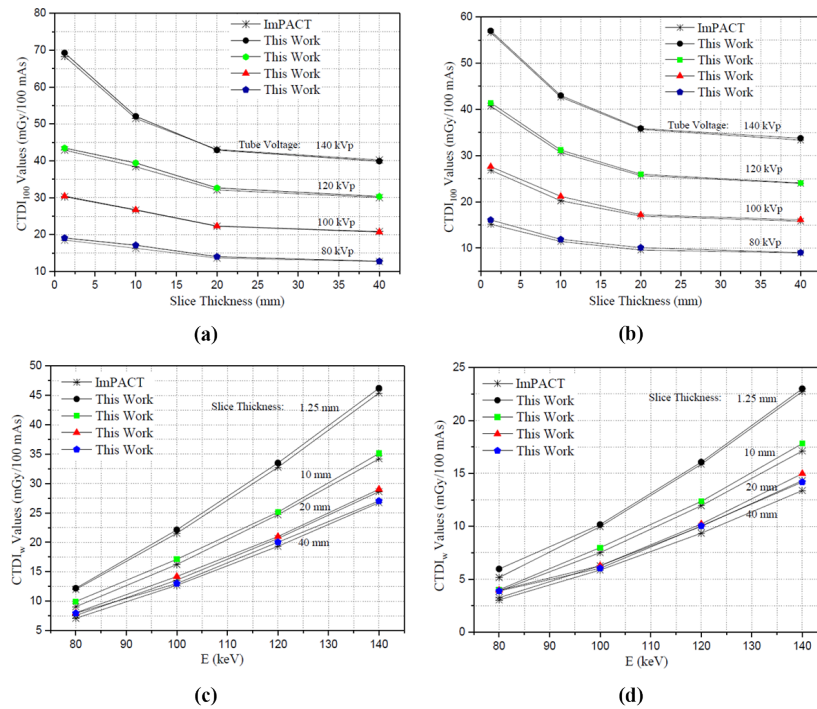


Figure 4: Mean free-in-air computed tomography dose index values as a function of different tube potentials and slice thicknesses for (a) small bowtie filter, and (b) large bowtie filter, computed tomography dose index values as a function of various tube voltages and beam widths for (c) head, and (d) body phantoms, comparing the ImPACT data, and our simulated data obtained by our developed CT simulator demonstrates 4.2% difference, averaged across all dose index values.

Table 2: Computed tomography dose index values in air and head and body dosimetry phantoms and standard deviations obtained under the same exposure condition indicated in Table 1, comparing our results and other previously published data.

Number	Work	CTDI _{air} Small bowtie filter	CTDI _{air} Large bowtie filter	CTDI _w Small bowtie filter	CTDI _w Large bowtie filter
1	Simulated Data	29.34±0.2	23.7±0.1	18.73±0.1	9.04±0.2
2	Experimented Data	28.03±0.3	23.01±0.5	17.92±0.4	8.62±0.5
3	†Imaging Performance Assessment of CT [15]	30.01	23.99	19.32	9.37
4	General Electric Manufacturer's data [16]	27.46±0.4	22.95±0.4	16.31±0.4	7.92±0.4
5	Experimental Published data [17]	29.5±0.5	23.8±0.3	18.1±0.3	8.9±0.1
	Difference (1 vs 2)	4.7%	3.0%	4.5%	4.9%
	Difference (1 vs 3)	2.3%	1.23%	3.1%	3.5%
	Difference (1 vs 4)	6.9%	3.3%	14.8%	14.14%
	Difference (1 vs 5)	0.54%	0.42%	3.48%	1.57%

†This reference has not revealed any standard deviation.

CTDI: Computed tomography dose index

MCNP-FBSM MC software package has been developed by the implementation of bowtie filters. In addition, extensive validation of our developed CT simulator has been made through the comparisons with our experimental results and a wide range of previously published reference data [15-17]. The minimum and maximum observed mean differences of our simulation results and other above-mentioned data were 1.5% and 9.79%. These variations can be attributed mainly to the different used X-ray spectra, the elemental composition of CTDI phantoms, errors introduced when ignoring the variabilities across tube current and voltage settings. According to the IAEA [30], the acceptable difference for radiation dose metric must be within $\pm 20\%$ of the reference values, and accordingly, all showed discrepancies between the results of the present study and other studies [15-17] that seem to be reasonable. Consequently, our developed CT simulator is a valid and beneficial tool for CT dosimetry.

Conclusion

CT is one of the most valuable diagnostic imaging tools in the clinic. However, a relatively high dose is delivered to the patient during CT imaging, and having an appropriate CT simulator is highly desired to estimate and optimize the absorbed radiation dose. In this work, a novel CT simulator was developed and extended based on MCNP-FBSM MC code, utilizing head and body bowtie filters for dosimetry applications. Extensive validation of the CT simulator was performed to check the accuracy of its outcomes, demonstrating very good agreement between our experimental acquired data and previously published data. Therefore, this CT simulator is an adequate platform for a wide range of research tasks such as the virtual evaluation and optimization of CT parameters.

Conflict of Interest

None

References

1. Johnson JO. Emergency imaging: case review e-book. Elsevier Health Sciences; 2019.
2. Khodajou-Chokami H, Hosseini SA, Ghorbanzadeh M, Mohammadi M. QCT: A Measuring Tool Dedicated to the Estimation of Image Parameters for Quality Assurance/Quality Control Programs of CT Scanners. International Symposium on Medical Measurements and Applications (MeMeA); Bari, Italy: IEEE; 2020. doi: 10.1109/MeMeA49120.2020.9137199.
3. Khursheed A, Hillier MC, Shrimpton PC, Wall BF. Influence of patient age on normalized effective doses calculated for CT examinations. *The Br J Radiol.* 2002;**75**(898):819-30. doi: 10.1259/bjr.75.898.750819. PubMed PMID: 12381691.
4. Ebrahimi-Khankook A, Akhlaghi P, Vejdani-Noghreiyani A. Studying the lung dose uncertainty during chest CT scans using phantoms with statistical lung volumes and shapes. *J Radiol Prot.* 2019;**39**(2):443-454. doi: 10.1088/1361-6498/ab0116. PubMed PMID: 30673649.
5. MCNP Monte Carlo Team. MCNP, a general Monte Carlo N-particle transport code. Los Alamos National Laboratory; 2020. Available from: <https://mcnp.lanl.gov/>.
6. Geant4 Working Groups and Coordinators. GEANT4, GEometry ANd Tracking, A simulation toolkit. 2020. Available from: <https://geant4.web.cern.ch/>.
7. FLUKA Monte Carlo Team. FLUKA, FLUKtuierende KAskade. 2020. Available from: <http://www.fluka.org/fluka.php>.
8. EGSnrc Monte Carlo Team. EGSnrc, Electron Gamma Shower. 2020. Available from: <https://github.com/nrc-cnrc/EGSnrc>.
9. Kostou T, Papadimitroulas P, Papaconstadopoulos P, Devic S, Seuntjens J, Kagadis GC. Size-specific dose estimations for pediatric chest, abdomen/pelvis and head CT scans with the use of GATE. *Phys Med.* 2019;**65**:181-90. doi: 10.1016/j.ejmp.2019.08.020. PubMed PMID: 31494372.
10. Kramer R, Cassola VF, Andrade ME, De Araújo MW, Brenner DJ, Houry HJ. Mathematical modelling of scanner-specific bowtie filters for Monte Carlo CT dosimetry. *Phys Med Biol.* 2017;**62**(3):781-809. doi: 10.1088/1361-6560/aa5343. PubMed PMID: 28072578.
11. Somasundaram E, Artz NS, Brady SL. Development and validation of an open source Mon-

- te Carlo dosimetry model for wide-beam CT scanners using Fluka. *J Appl Clin Med Phys*. 2019;**20**(4):132-47. doi: 10.1002/acm2.12559. PubMed PMID: 30851155. PubMed PMCID: PMC6448170.
12. Akhavanallaf A, Xie T, Zaidi H. Assessment of uncertainties associated with Monte Carlo-based personalized dosimetry in clinical CT examinations. *Phys Med Biol*. 2020;**65**(4):045008. doi: 10.1088/1361-6560/ab6b45. PubMed PMID: 31935713.
 13. Khodajou-Chokami H, Hosseini SA, Ay MR, Zaidi H. Mncp-fbsm: Development of mncp/mc-npx source model for simulation of multi-slice fan-beam x-ray ct scanners. International Symposium on Medical Measurements and Applications (MeMeA); Istanbul, Turkey: IEEE; 2019.
 14. International Electrotechnical Commission. Medical electrical equipment-X-ray tube assemblies for medical diagnosis-Characteristics of focal spots. 4th Edition. IEC; 2005.
 15. ImPACT 2004. GE LightSpeed16 CT scanner technical evaluation imaging performance assessment of CT scanners group. 2020. Available from: <http://www.impactscan.org/ctdosimetry.htm>.
 16. GE Healthcare. LightSpeed™ VCT Technical Reference Manual. General Electric Company; 2011.
 17. Mathieu KB, McNitt-Gray MF, Zhang D, Kim HJ, Cody DD. Precision of dosimetry-related measurements obtained on current multidetector computed tomography scanners. *Med phys*. 2010;**37**(8):4102-9. doi: 10.1118/1.3426000. PubMed PMID: 20879570. PubMed PMCID: PMC2917455.
 18. Khodajou-Chokami H, Hosseini SA, Ay MR, Sa-farzadehamiri A, Ghafarian P, Zaidi H. A novel method for measuring the mtf of ct scanners: A phantom study. International Symposium on Medical Measurements and Applications (MeMeA); Istanbul, Turkey: IEEE; 2019.
 19. Pelowitz DB. MCNPX USER'S MANUAL Version 2.7. 0-LA-CP-11-00438. Los Alamos National Laboratory; 2011. Available from: https://mncp.lanl.gov/pdf_files/la-ur-11-02295.pdf.
 20. Storm E, Israel HI. Photon cross sections from 0.001 to 100 MeV for elements 1 through 100. New Mexico, Los Alamos Scientific Lab; 1967. Available from: <https://digital.library.unt.edu/ark:/67531/metadc1034104/>.
 21. Hubbell JH, Veigele WJ, Briggs EA, Brown RT, Cromer DT, Howerton DR. Atomic form factors, incoherent scattering functions, and photon scattering cross sections. *J Phys Chem Ref Data*. 1975;**4**(3):471-538. doi: 10.1063/1.555523.
 22. Cullen DE, Hubbell JH, Kissel L. EPDL97: the evaluated photo data library 97 version. CA (United States): Lawrence Livermore National Lab; 1997.
 23. Khodajou-Chokami H, Vahdat BV, Ebrahimi-Khankook A, Noorvand M. MamSim: A Computational Software Platform for Measuring and Optimizing Imaging and Dosimetry Parameters in Screen-Film and Digital Mammography Systems. International Symposium on Medical Measurements and Applications (MeMeA); Bari, Italy: IEEE; 2020.
 24. Punnoose J, Xu J, Sisniega A, Zbijewski W, Siewerdsen JH. spektr 3.0—A computational tool for x-ray spectrum modeling and analysis. *Med Phys*. 2016;**43**(8Part1):4711-7. doi: 10.1118/1.4955438. PubMed PMID: 27487888. PubMed PMCID: PMC4958109.
 25. Boone JM, Seibert JA. An accurate method for computer-generating tungsten anode x-ray spectra from 30 to 140 kV. *Med Phys*. 1997;**24**(11):1661-70. doi: 10.1118/1.597953. PubMed PMID: 9394272.
 26. Cranley K, Gilmore BJ, Fogarty GWA, Deponds L. Catalog of diagnostic X-ray spectra and other data. IPEM report no. 78; IPEM Publications; 1997.
 27. Birch R, Marshall M. Computation of bremsstrahlung x-ray spectra and comparison with spectra measured with a Ge (Li) detector. *Phys Med Biol*. 1979;**24**(3):505. doi: 10.1088/0031-9155/24/3/002. PubMed PMID: 461510.
 28. Gu J, Bednarz B, Caracappa PF, Xu XG. The development, validation and application of a multi-detector CT (MDCT) scanner model for assessing organ doses to the pregnant patient and the fetus using Monte Carlo simulations. *Phys Med Biol*. 2009;**54**(9):2699. doi: 10.1088/0031-9155/54/9/007. PubMed PMID: 19351983. PubMed PMCID: PMC3376893.
 29. Boone JM. Method for evaluating bow tie filter angle-dependent attenuation in CT: Theory and simulation results. *Med Phys*. 2010;**37**(1):40-8. doi: 10.1118/1.3264616. PubMed PMID: 20175464. PubMed PMCID: PMC2801732.
 30. McLean ID. Quality assurance programme for

- computed tomography: diagnostic and therapy applications. IAEA Human Health Series No. 19; IAEA; 2012.
31. European Commission. European Guidelines on Quality Criteria for Computed Tomography. EUR 16262 EN; Luxemburg Office for Official Publications of the European Communities; 1999. Available from: <http://www.drs.dk/guidelines/ct/quality/Page032.htm>.
32. Hubbell JH, Seltzer SM. Tables of X-ray mass attenuation coefficients and mass energy-absorption coefficients 1 keV to 20 MeV for elements Z= 1 to 92 and 48 additional substances of dosimetric interest. National Inst; 1995. Available from: <http://physics.nist.gov/PhysRefData/Xray-MassCoef/cover.html>.